NANO LETTERS

Letter

pubs.acs.org/NanoLett

Highly Conductive Single-Molecule Wires with Controlled Orientation by Coordination of Metalloporphyrins

Albert C. Aragonès,[†,‡,¶] Nadim Darwish,[†,¶] Wojciech J. Saletra,[§] Lluïsa Pérez-García,[∥,⊥] Fausto Sanz,[†,‡] Josep Puigmartí-Luis,[*,§,#] David B. Amabilino,[*,§] and Ismael Díez-Pérez[*,†]

[†]Departament de Química Física, Universitat de Barcelona, Diagonal 645, and Institut de Bioenginyeria de Catalunya (IBEC), Baldiri Reixac 15-21, 08028 Barcelona, Catalonia, Spain

[‡]Centro Investigación Biomédica en Red (CIBER-BBN), Campus Río Ebro-Edificio I+D, Poeta Mariano Esquillor s/n, 50018 Zaragoza, Spain

[§]Institut de Ciència de Materials de Barcelona (ICMAB-CSIC), Campus Universitari, 08193 Bellaterra, Catalonia, Spain

[∥]Facultat de Farmàcia, Universitat de Barcelona, 08028 Barcelona, Catalonia, Spain

[⊥]Institut de Nanociència i Nanotecnologia, Universitat de Barcelona, 08028 Barcelona, Catalonia, Spain

[#]Empa, Laboratory for Protection and Physiology, Lerchenfeldstrasse 5, 9014 St. Gallen, Switzerland

Supporting Information

ABSTRACT: Porphyrin-based molecular wires are promising candidates for nanoelectronic and photovoltaic devices due to the porphyrin chemical stability and unique optoelectronic properties. An important aim toward exploiting single porphyrin molecules in nanoscale devices is to possess the ability to control the electrical pathways across them. Herein, we demonstrate a method to build single-molecule wires with metalloporphyrins via their central metal ion by chemically modifying both an STM tip and surface electrodes with pyridin-4-yl-methanethiol, a molecule that has strong affinity for coordination with the metal ion of the porphyrin. The new flat configuration resulted in single-molecule junctions of exceedingly high lifetime and of conductance 3 orders of magnitude larger than that obtained previously for similar porphyrin molecules but wired from either end of the porphyrin ring. This work presents a new concept of building highly efficient single-molecule electrical contacts by exploiting metal coordination chemistry.

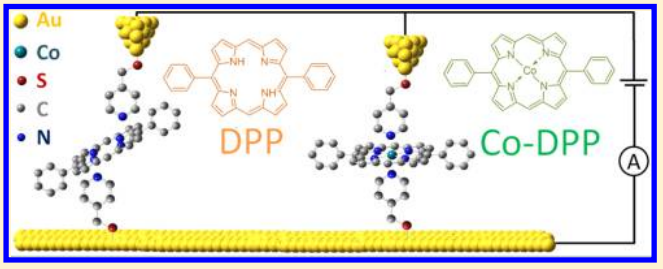

KEYWORDS: *single-molecule wires, coordinating individual metalloporphyrins, controlled molecular orientation, optimized coupling by axial coordination*

Inspired by the proposal that single molecules will be functional parts of future electronic devices, there exists a considerable interest in understanding charge transport across them, both experimentally and theoretically.[1−8] One of the numerous molecular systems that hold great promise in this area is porphyrins, partly because of their well-developed synthetic routes by which a variety of chemical substituents and central metal ions can be introduced in their structure to tune their electrical properties. Porphyrin derivatives play a vital role in charge separation that take place in naturally occurring photosynthetic processes and in metalloproteins involved in the respiratory chain,[9−13] and it is envisioned that they can play an important role in future artificial electronic devices.[14−16] For these reasons, it is critical to understand and control charge transport through porphyrins, which is a process largely dictated by the electrode−molecule orientation and the porphyrin−electrode chemical contacts during measurements.

Recent studies using the scanning tunneling microscope (STM) break-junction technique[1] showed that the conductance of a single porphyrin covalently bond in an upright configuration is significantly affected by the binding contact geometry, the employed chemical anchoring groups and the coupling ability of the π orbitals to the metallic leads.[17−23] Porphyrin junctions in such a configuration were shown to exhibit unique characteristics such as a very shallow decay of conductance with length ($\beta = 0.04$ Å^{-1}).[17,18] In these previous studies, the supramolecular backbones of the porphyrins were modified synthetically to allow their attachment to the electrodes, usually gold, via a suitable linker such as thiols and pyridines.[19,20] The strong affinity of such contact groups to the gold electrodes together with the rigid structure of the porphyrin backbone is anticipated to yield restricted junction configurations. Thus, the configuration of the single-molecule junctions formed from porphyrins is commonly represented as being straight and perpendicular to the electrodes[17−21] (Figure 1a). These built-in chemical contacts were

Received: May 21, 2014
Revised: June 24, 2014

   dx.doi.org/10.1021/nl501884g | *Nano Lett.* XXXX, XXX, XXX−XXX

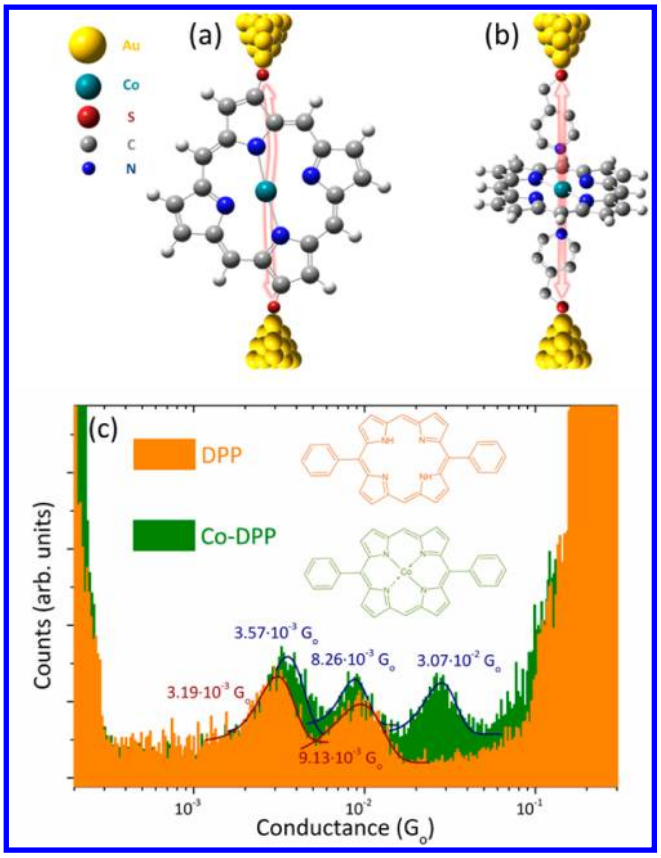

Figure 1. (a) Representation of the common upright configuration for single porphyrin conductance experiments. (b) Schematic representation of the flat configuration investigated in this work. (c) Semilog conductance histograms for the DPP molecule (orange) and Co-DPP molecule (green) using the junction configuration represented in panel b. The conductance values are extracted from Gaussian fits of the peaks.

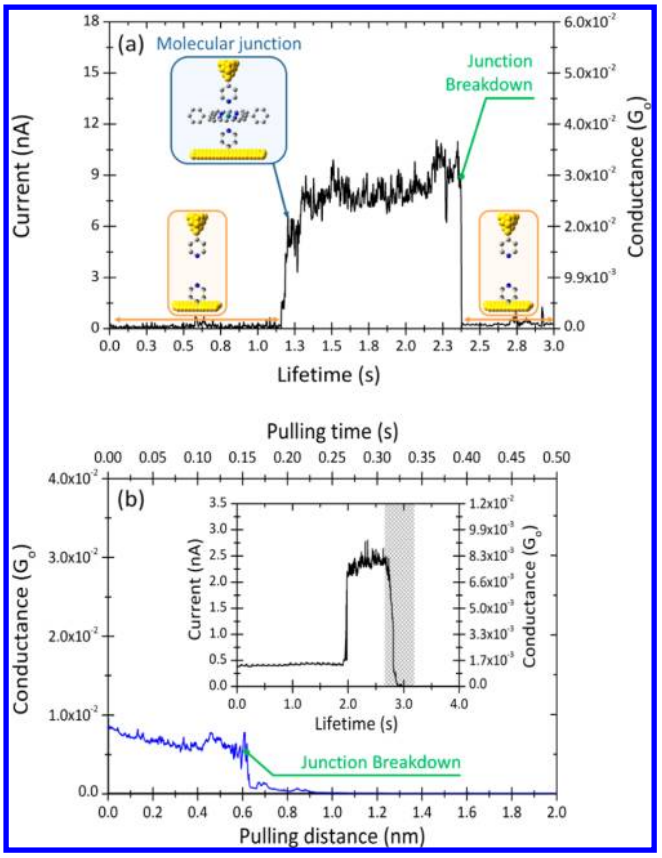

Figure 2. (a) Representative "*blink*" due to the spontaneous formation of a single-molecule junction with the Co-DPP molecule; the current decays suddenly due to either spontaneous or induced breakdown of the junction. Tip-to-sample distance was initially set by a 4 nA set point current and normalized to zero in the plot. (b) Shows an induced STM tip pulling curve of the inset blink (the shadowed area indicates the pulling stage) for the Co-DPP molecule.

successful for studying charge transport along the length of the porphyrin backbone and pave the way to the investigation of other interesting junction configurations such as the porphyrin oriented flat between the electrodes. Such a new configuration mimics the electron transport across porphyrins in naturally occurring phenomena such as photosynthetic and transmembrane electron transport.[11,12] In these natural processes, the common orientation of the porphyrin ring is perpendicular to the main pathway of electrons or energy through an axial coordination of chemical ligands with the metal center of the porphyrin molecule.[12,13]

In this study, we present a new approach to form single molecular junctions with porphyrin molecules. Namely, we chemically modify both the gold STM tips and Au (111) surfaces with pyridin-4-yl-methanethiol allowing porphyrin molecules introduced in the solution to close the circuit between the STM tip and the gold surface through metal−pyridine coordination (Figure 1b). We utilize the STM junction technique in its two common approaches, break-junction[1] and spontaneous formation of molecular junctions,[24] to determine the single molecular conductance. Further, we investigate the effect of the tip−surface distance on the conductance magnitude and the duration (lifetime) of the molecular junctions. We then propose molecular models that describe the experimental findings based on DFT optimized geometries and distribution of frontier orbitals of the most stable molecular configurations between the electrodes.

Two molecules were used in this study, a free base porphyrin, 5,15-diphenylporphyrin (DPP), which has no metallic center and therefore no strong interaction with the pyridinyl groups on the electrode surfaces, and a metalloporphyrin Co(II)-5,15-diphenylporphyrin (Co-DPP) with a divalent cobalt center, which allows coordination[25] to pyridinyl ligands affording a hexacoordinate system.[26−28] Initially, the STM break-junction approach[1] was used to determine the single-molecule conductance of each molecule. Conductance histograms (Figure 1c) were built by the accumulation of hundreds of individual pulling traces and the peak maxima represent the most probable conductance values (see Supporting Information section 9 for details).

In the conductance histograms, both the DPP molecule and the Co-DPP share two conductance levels, a low conductance (**LC**) level at ca. 3×10^{-3} G_o and a medium conductance (**MC**) level at ca. 9×10^{-3} G_o. Unlike the DPP molecule, the Co-DPP shows an extra high conductance (**HC**) level at ca. 3×10^{-2} G_o. This **HC** value is about 3 orders of magnitude higher than that obtained previously from porphyrin molecules of comparable length to the Co-DPP molecule, but directly connected to the electrodes in an upright configuration.[18,21]

In order to understand the origin of the multiple conductance peaks observed in the break-junction experiments of Figure 1c, we carried out current transient captures at a fixed distance such that spontaneous formation of molecular junctions is attained.

dx.doi.org/10.1021/nl501884g | *Nano Lett.* XXXX, XXX, XXX−XXX

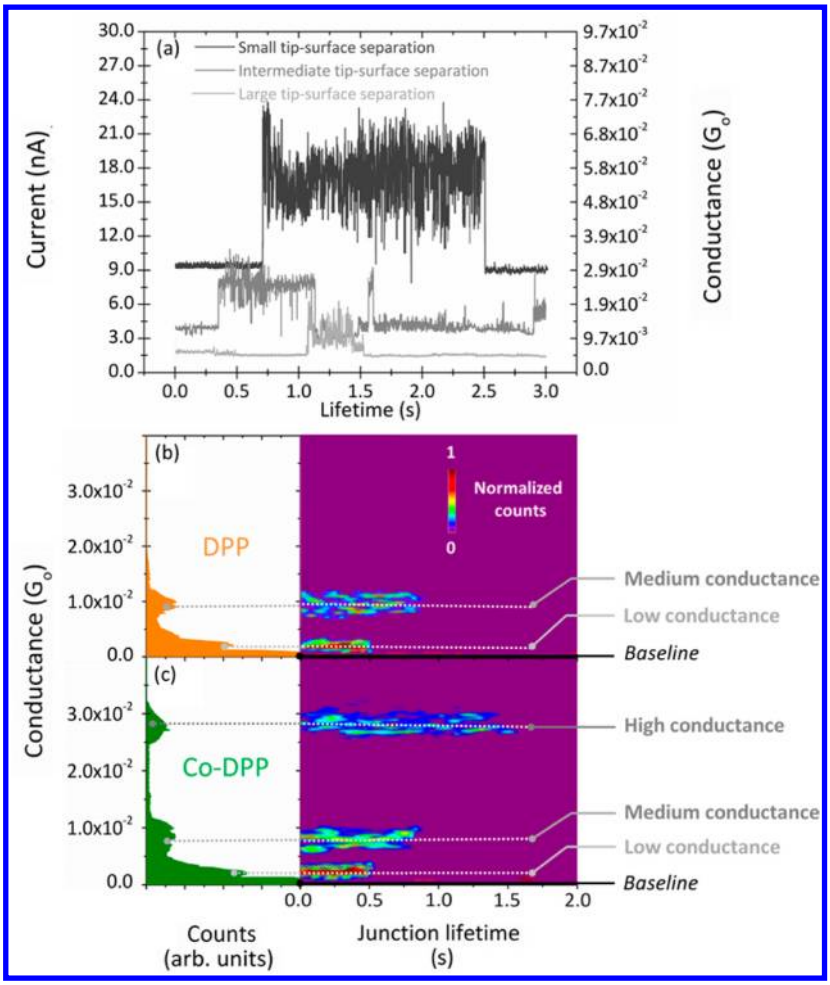

Figure 3. (a) Representative individual "*blinks*" corresponding to the formation of molecular junctions with the Co-DPP molecule at three different tip-to-surface distances determined by 2, 4, and 9 nA set point currents for large, intermediate, and small separations, respectively. (b,c) 1D conductance histograms (left panel) and the corresponding 2D maps (right panel) obtained from tens of *blinking* traces for (b) DPP and (c) Co-DPP. Counts (color legend) have been normalized versus the total amount of counts and a scale of one (100%) has been set for the maximum normalized value.

Briefly, imposing a set point tunneling current first sets an initial distance between the functionalized electrodes. The STM feedback is then turned off and the tunneling current is recorded as a function of time (Figure 2a). When a molecular junction is spontaneously formed, the current suddenly jumps. We refer to these current jumps as "*blinks*" and this type of experiments as the *blinking experiments*. The blink in this study corresponds to a molecular bridge formation between the pyridine-functionalized electrodes and the porphyrin molecule. The blinks typically last for a short period of time, after which the current suddenly drops due to the spontaneous breakdown of the junction. In order to ensure that the recorded blinks are due solely to the formation of molecular junctions, a mechanical induced STM tip pulling procedure[29] was eventually applied during the lifetime of the blinks (Figure 2b). The appearance of plateaus as the junction is mechanically forced to break evidence that the blink was due to the formation of a molecular bridge. Conversely, pulling the STM tip during the absence of a blink showed a fast exponential decay confirming the correlation between the appearance of blinks and the formation of molecular bridges (see details in Supporting Information section 1). Unlike the STM break-junction approach, which forces the tip in and out of the surface and therefore may lead to stretch-dependent conductance, the spontaneous formation of junctions (blinking approach) could be envisioned as a method to momentarily freeze particular conformations in the single-molecule junction.[24,30] More importantly, the blinking approach can provide reliable information about the lifetime and therefore the strength of the electrode-molecule interaction.

Typical blinking traces are shown in Figure 3a at different tip-to-surface separations. The statistical analysis of the measured conductances from the blinking traces is obtained from building 1D conductance histograms and 2D maps from tens of blinks (Figure 3b and 3c). Consistent with the values obtained from the STM break-junction experiments (Figure 1c), the DPP molecule showed **LC** and **MC** levels around 3×10^{-3} and 9×10^{-3} G_o, respectively. Likewise, the Co-DPP molecule showed, in addition to the **LC** and **MC** level, an extra **HC** level around 3×10^{-2} G_o. Note that the initial set point currents (baselines levels in Figure 3a) were set high (above 2 nA, see Supporting Information section 1) such as the tip and substrate are separated by short distances to promote "lying flat" conformations of the porphyrin between the electrodes, resulting in the measured high conductances (see control experiments in Supporting Information sections 3 and 4). The lifetime of the blinks was highest for the **HC,** followed by the **MC** and the shortest blinks were that for the **LC** (see details in Supporting Information section 2). The average lifetime of the **HC** blinks is 1.5 s at small tip-to-surface

dx.doi.org/10.1021/nl501884g | *Nano Lett.* XXXX, XXX, XXX−XXX

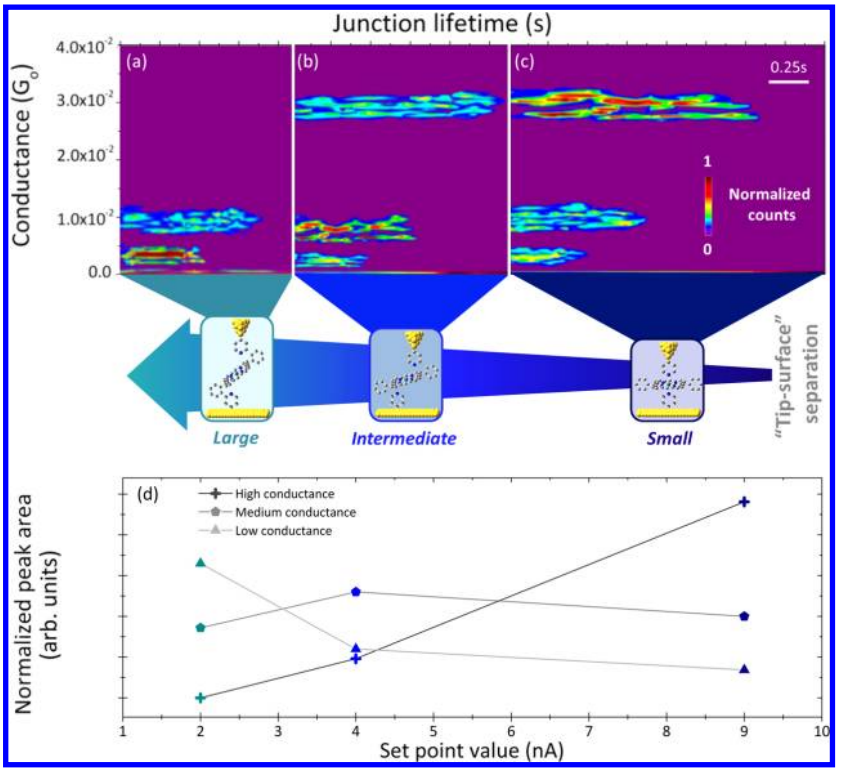

Figure 4. 2D *blinking* maps at three different tip-to-surface separations for the pyridinyl-coordinated Co-DPP junction at (a) large separation (2 nA set point current), (b) intermediate separation (4 nA set point current) and (c) small separation (9 nA set point current). The estimated decrease in the tip-to-substrate distance when going from (a) to (c) is ∼0.9 nm (see Supporting Information section 1). (d) Plot of the normalized peak area of the 1D histograms in (a)−(c) (see Supporting Information section 5) versus current set point values (increasing set point means decreasing tip-to-surface separation). To allow comparison among (a)−(c), counts (color legend) have been normalized versus the total amount of counts among all three maps and a scale of 1 (100%) for the maximum normalized value has been set.

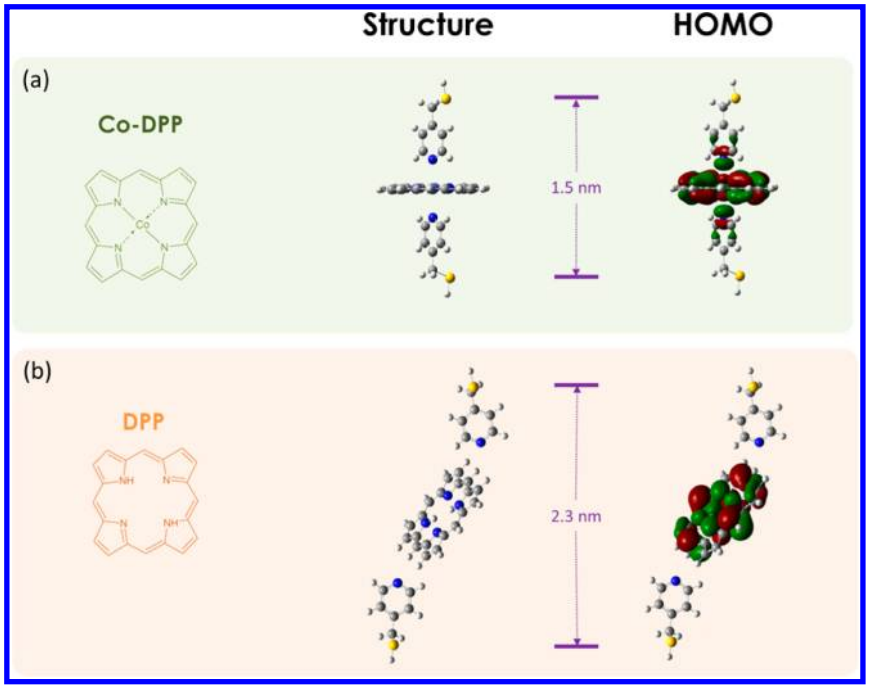

Figure 5. Molecular structure and DFT optimized geometry together with the HOMO frontier orbital of (a) the pyridine−Co-DPP−pyridine axial coordination and (b) the pyridine−DPP−pyridine coordination. The phenyl rings have been omitted for simplicity (see Supporting Information section 7).

gap distances, which suggests that the molecular junction configuration leading to the **HC** blinks are significantly more stable. Blinking experiments in the absence of porphyrin molecules or in the absence of the pyridinyl units at the electrodes showed no blinking events under the same experimental conditions (see details in Supporting Information

dx.doi.org/10.1021/nl501884g | *Nano Lett.* XXXX, XXX, XXX−XXX

section 3 and 4). Thus, the presence of the **HC** level for the Co-DPP and its absence in the DPP in both the break-junction and the blinking experiments evidence that the Co center is directly involved in the molecular junction formation with Co-DPP molecules via hexacoordination of the Co metal center with the two nitrogen atoms in the pyridinyl units present on both the surface and the STM tip electrodes (Figure 1b). The transition from tetra to hexacoordinated Co with the two pyridine-modified electrodes gives rise to the extra high conductance level observed for the Co-DPP. Examples of similar high conductive molecular wires induced by a metallorganic redox moiety inserted into a molecular backbone have been previously reported.[31,32]

Further investigation of the origin of the three conductance levels (**LC**, **MC** and **HC**) was obtained by analyzing blinks for the Co-DPP molecule at different tip−surface gap separations. Figure 4a−c shows 2D maps built from tens of blinks recorded at different initial set point currents. The change in the number of bands (conductance levels) and their intensity (color counts) at the different set points indicates the propensity to stabilize particular molecular conformations as a function of the tip-to-surface separation. Namely, when the tip-to-surface separation is large, the most frequently observed blinks are the **LC** ones (see color counts in Figure 4a). As the tip-to-surface distance diminishes, the **MC** level dominates at intermediate distances, whereas the **HC** level dominates at the smallest separations (see color counts in Figure 4b−c and representative blinks in Figure 3a). The trends are observed by representing the normalized counts (see Supporting Information sections 5 and 6) of all three levels of conductance as a function of the tip-to-surface separation (Figure 4d). Note that the junction lifetimes are comparable for all three tip-to-surface separations, except for a slight (~0.25 s) increase in the **HC** junction lifetime when going from intermediate to small tip-to-surface separations. This last trend may suggest a partially strained hexacoordinated Co-DPP junction in the case of intermediate distances that results in premature force-induced junction breakdown decreasing the overall complex stability.

The distance-dependence of the **HC** blinks strongly suggests that they originate from molecular junctions through the cobalt coordination. Co coordination to the pyridine units requires the porphyrin molecule to be oriented flat at the junction (Figure 1b) with shorter pyridine-to-Co distance. Such a configuration is more likely to occur at small tip-to-surface separations (Figure 4c−d). This flat configuration is supported by geometry optimization of a pyridine−Co-DPP−pyridine junction using density functional theory (DFT-B3LYP) methods (see Supporting Information section 7), which revealed the formation of a hexacoordinated Co with the two pyridinyl moieties approaching the Co center at Co−N distances of less than 2 Å (Figure 5a center panel). This is consistent with the values obtained from X-ray crystal structures of Pyridine−Co−porphyrin−Pyridine complexes.[15] The strong Co−pyridine interaction is also demonstrated by the generation of delocalized HOMO orbitals along the pyridine−Co−pyridine axis (Figure 5a right panel). We attribute the **HC** level to the generated extended electronic pathway between the two electrodes by the molecular orbital delocalization along the junction main axis as a consequence of the pyridine−Co−pyridine coordination.

The **LC** and **MC** conductance levels that are common for both the DPP and the Co-DPP molecules can be explained by hydrogen bonding interactions between the pyridine units and the backbone of the porphyrin molecule that could happen at multiple sites. This hypothesis is supported by geometry optimization for the pyridine−DPP−pyridine adduct, which results in multiple configurations with the two pyridinyl groups forming H-bonds at different sites of the porphyrin (see representative H-bonding configurations in Figure 5b and Supporting Information section 7). Recent works have also suggested the possibility of wiring two electrodes through H-bonding interactions.[33,34] Hydrogen bonds can occur in geometries such that the porphyrin ring is highly tilted resulting in a much longer S-to-S junction (see Supporting Information section 7). These multiple long-distance interactions can be correlated with the dominance of the **LC** and the **MC** levels at larger tip-to-surface separations. The HOMO and LUMO levels of these H-bonding configurations are mostly localized on the porphyrin moiety (see Figure 5b right panel), with orbital-distribution similar to those obtained from the isolated porphyrin. The absence of delocalized orbitals along the pyridine−DDP−pyridine axis is an accord with the absence of **HC** level in the DPP junctions. The increase in the junction distance from Figure 5a to b is in qualitatively agreement with the estimated increase of tip-to-substrate distance when going from high to low set point values in Figure 4 (see Supporting Information section 1). It is important to note that in Figure 5b the electrode−electrode separation has been increased in the DFT optimization to identify possible interactions at large distances. However, H-bonding interactions can occur at a rather wide range between the H-donor and the H-acceptor[35] (Supporting Information Figure S6b top panel) and, therefore, H-bonding can also take place at the lower tip-to-surface separations such as that depicted in Figure 5a, as observed experimentally (see Figure 4c).

The approach outlined herein offers a control over the contact of porphyrin molecules in single-molecule circuitry such that previously inaccessible electronic pathways across the porphyrin can be achieved. This is made possible by "catching" the porphyrin molecule by its metallic center using coordination chemistry. We show that by changing the STM tip−surface distance we can alter the configuration of the junction and the binding sites and consequently control the conductance output of the single-molecule device. Of a particular note is the demonstration that by decreasing the STM tip−surface distance, the chances of wiring the porphyrin molecule from its metal center increase and, consequently, lead to a highly stable and highly conductive molecular wire. This high conductivity is attributed to the efficient electronic pathway via the metallic center of the porphyrin. We expect this general approach to be of a broader usage in the design of single-molecule devices that exploit coordination chemistry to achieve site-directed molecule−electrode connectivity.

■ ASSOCIATED CONTENT

Ⓢ Supporting Information

Experimental details on sample preparation and single-molecule transport experiments, control experiments of the single-molecule transport measurements and computational details. This material is available free of charge via the Internet at http://pubs.acs.org.

■ AUTHOR INFORMATION

Corresponding Authors

*E-mail: isma_diez@ub.edu.
*E-mail: amabilino@icmab.es.
*E-mail: josep.puigmarti@empa.ch.

dx.doi.org/10.1021/nl501884g | *Nano Lett.* XXXX, XXX, XXX−XXX

Author Contributions

[¶]A.C.A. and N.D. contributed equally

Notes

The authors declare no competing financial interest.

■ ACKNOWLEDGMENTS

A.C.A. thanks the Spanish Ministerio de Educación, Cultura y Deporte for a graduate FPU fellowship. N.D. acknowledges the European Union for a Marie Curie IIF Fellowship. This research was supported by national projects CTQ2012-36090, CTQ2010-16339, and 2009 SGR 158 and EU Reintegration Grant (FP7-PEOPLE-2010-RG-277182). I.D.-P. and J.P.-L. thank the Ramon y Cajal program (MINECO, RYC-2011-07951 and RYC-2011-08071) for financial support.

■ REFERENCES

(1) Xu, B.; Tao, N. J. *Science* **2003**, *301*, 1221−1223.
(2) Nichols, R. J.; Haiss, W.; Higgins, S. J.; Leary, E.; Martin, S.; Bethell, D. *Phys. Chem. Chem. Phys.* **2010**, *12*, 2801−2815.
(3) Tao, N. J. *Nat. Nanotechnol.* **2006**, *1*, 173−181.
(4) Chen, F.; Tao, N. J. *Acc. Chem. Res.* **2009**, *42*, 429−438.
(5) Bürkle, M.; Viljas, J.; Vonlanthen, D.; Mishchenko, A.; Schön, G.; Mayor, M.; Wandlowski, T.; Pauly, F. *Phys. Rev. B: Condens. Matter Mater. Phys.* **2012**, *85*, 075417−12.
(6) Bürkle, M.; Zotti, L. A.; Viljas, J. K.; Vonlanthen, D.; Mishchenko, A.; Wandlowski, T.; Mayor, M.; Schön, G.; Pauly, F. *Phys. Rev. B: Condens. Matter Mater. Phys.* **2012**, *86*, 115304−8.
(7) Aradhya, S. V.; Venkataraman, L. *Nat. Nanotechnol.* **2013**, *8*, 399−410.
(8) Darwish, N.; Paddon-Row, M. N.; Gooding, J. J. *Acc. Chem. Res.* **2013**, *47*, 385−395.
(9) McDermott, G.; Prince, S. M.; Freer, A. A.; Hawthornthwaite-Lawless, A. M.; Papiz, M. Z.; Cogdell, R. J.; Isaacs, N. W. *Nature* **1995**, *374*, 517−521.
(10) Zhang, Z.; Huang, L.; Shulmeister, V. M.; Chi, Y. I.; Kim, K. K.; Hung, L. W.; Crofts, A. R.; Berry, E. A.; Kim, S. H. *Nature* **1998**, *392*, 677−84.
(11) Regan, J. J.; Ramirez, B. E.; Winkler, J. R.; Gray, H. B.; Malmström, B. G. *J. Bioenerg. Biomembr.* **1998**, *30*, 35−39.
(12) Gray, H. B.; Winkler, J. R. *Biochim. Biophys. Acta* **2010**, *1797*, 1563−72.
(13) Allen, J. W.; Watmough, N. J.; Ferguson, S. J. *Nat. Struct. Biol.* **2000**, *7*, 885−888.
(14) Liu, Z.; Yasseri, A. A.; Lindsey, J. S.; Bocian, D. F. *Science* **2003**, *302*, 1543−1545.
(15) Dey, S.; Ikbal, S. A.; Rath, S. P. *New J. Chem.* **2014**, DOI: 10.1039/C3NJ01248D.
(16) Lee, J. T.; Chae, D.-H.; Yao, Z.; Sessler, J. L. *Chem. Commun.* **2012**, *48*, 4420−4422.
(17) Sedghi, G.; Sawada, K.; Esdaile, L. J.; Hoffmann, M.; Anderson, H. L.; Bethell, D.; Haiss, W.; Higgins, S. J.; Nichols, R. J. *J. Am. Chem. Soc.* **2008**, *130*, 8582−8583.
(18) Sedghi, G.; García-Suárez, V. M.; Esdaile, L. J.; Anderson, H. L.; Lambert, J. C.; Martín, S.; Bethel, D.; Higgins, S. J.; Elliott, M.; Bennett, N.; Macdonald, J. E.; Nichols, R. J. *Nat. Nanotechnol.* **2011**, *6*, 517−523.
(19) Li, Z.; Smeu, M.; Ratner, M. A.; Borguet, E. *J. Phys. Chem. C* **2013**, *117*, 14890−14898.
(20) Li, Z.; Borguet, E. *J. Am. Chem. Soc.* **2011**, *134*, 63−66.
(21) Simbeck, A. J.; Qian, G.; Nayak, S. K.; Wang, G.-C.; Lewis, K. M. *Surf. Sci.* **2012**, *606*, 1412−1415.
(22) Perrin, M. L.; Prins, F.; Martin, C. A.; Shaikh, A. J.; Eelkema, R.; van Esch, J. H.; Briza, T.; Kaplanek, R.; Kral, V.; van Ruitenbeek, J. M.; van der Zant, H. S. J.; Dulic, D. *Angew. Chem.* **2011**, *123*, 11419−11422.
(23) Perrin, M. L.; Martin, C. A.; Prins, F.; Shalkh, A. J.; Eelkema, R.; van Esch, J. H.; van Ruitenbeek, J. M.; van der Zant, H. S. J.; Dulic, D. *Beilstein J. Nanotechnol.* **2011**, *2*, 714−719.
(24) Haiss, W.; Nichols, R. J.; van Zalinge, H.; Higgins, S. J.; Bethell, D.; Schiffrin, D. J. *Phys. Chem. Chem. Phys.* **2004**, *6*, 4330−4337.
(25) *Ionic Interactions in Natural and Synthetic Macromolecules*; Ciferri, A., Perico, A., Eds.; John Wiley & Sons, Inc.: Hoboken, NJ, 2012; p 337−359, DOI:10.1002/9781118165850.
(26) Corden, B. B.; Drago, R. S.; Perito, R. P. *J. Am. Chem. Soc.* **1985**, *107*, 2903−2907.
(27) Arnold, L.; Norouzi-Arasi, H.; Wagner, M.; Enkelmann, V.; Müllen, K. *Chem. Commun.* **2011**, *47*, 970−972.
(28) Wong, W.-Y. *Coord. Chem. Rev.* **2005**, *249*, 971−997.
(29) Diez-Perez, I.; Hihath, J.; Hines, T.; Wang, Z.-S.; Zhou, G.; Müllen, K.; Tao, N. *Nat. Nanotechnol.* **2011**, *6*, 226−31.
(30) Artés, J. M.; Díez-Pérez, I.; Gorostiza, P. *Nano Lett.* **2012**, *12*, 2679−84.
(31) Getty, S. A.; Engtrakul, C.; Wang, L.; Liu, R.; Ke, S.-H.; Baranger, H. U.; Yang, W.; Fuhrer, M. S.; Sita, L. R. *Phys. Rev. B: Condens. Matter Mater. Phys.* **2005**, *71*, 241401−4.
(32) Sun, Y.-Y.; Peng, Z.-L.; Hou, R.; Liang, J.-H.; Zheng, J.-F.; Zhou, X.-Y.; Zhou, X.-S.; Jin, S.; Niu, Z.-J.; Mao, B.-W. *Phys. Chem. Chem. Phys.* **2014**, *16*, 2260−2267.
(33) Zhao, Y.; Ashcroft, B.; Zhang, P.; Liu, H.; Sen, S.; Song, W.; Im, J.; Gyarfas, B.; Manna, S.; Biswas, S.; Borges, C.; Lindsay, S. *Nat. Nanotechnol.* **2014**, *9*, 466−473.
(34) Bui, P. T.; Nishino, T. *Phys. Chem. Chem. Phys.* **2014**, *16*, 5490−5494.
(35) Jeffrey, G. A. An introduction to hydrogen bonding. In *Topics in Physical Chemistry*, 1st ed.; Oxford University Press: New York, 1997.